scientific reports

Check for updates

OPEN

Oral andrographolide loaded lipid nanocarriers alleviate stress behaviors and hippocampal damage in TNF alpha induced neuroinflammatory mice

Sarawut Lapmanee[1,2], Natchanon Rimsueb[3], Phichaporn Bunwatcharaphansakun[3], Katawut Namdee[3], Prapimpun Wongchitrat[4], Sakkarin Bhubhanil[2], Nattapon Supkamonseni[2], Natthawut Charoenphon[5], Anjaree Inchan[6], Rattaporn Saenmuangchin[3] & Mattaka Khongkow[3]✉

This study aimed to improve the delivery efficacy of andrographolide (Andro) by encapsulating it in nanostructured lipid carriers (NLCs) and to evaluate its effectiveness in reducing systemic inflammation. These AndroNLCs exhibited homogeneity with a particle size of 131.40 ± 1.30 nm and approximately 89% encapsulation efficiency. AndroNLCs potentially enhanced oral efficacy by improving gastrointestinal stability, with reduced toxicity and inflammation in SH-SY5Y neuroblastoma cells. Inflammation was induced in sexually active C57BL/6 male mice with five intraperitoneal doses of 63 µg/kg TNF-alpha every three days. This was accompanied by daily oral administration of 10 mg/kg AndroNLCs, venlafaxine, or 1 mg/kg dexamethasone for 14 days. Mice with TNF-alpha-induced inflammation showed sickness signs and abnormal behaviors, assessed via physical changes, anxiety and depression tests (i.e., open field, elevated-T maze, tail suspension, and forced swimming), and biochemical assays. These changes included weight loss and compensatory responses to inflammation, as indicated by increased immune- and stress-modulated organ weights, elevated serum corticosterone levels, altered liver function markers, and higher levels of hippocampal IL-6 and TNF-alpha. Furthermore, histological analysis showed pyknotic cells, reduced layer thickness, and decreased hippocampal cell survival. Conversely, AndroNLCs significantly improved stress- and inflammation-related markers, alleviated behavioral abnormalities, reduced liver toxicity, and restored hippocampal morphology, showing effects greater than Andro alone and comparable to traditional treatments. These findings suggest that AndroNLCs have therapeutic effects on neuroinflammation but may risk contributing to mood disorders.

Keywords Andrographolide, Inflammation, Nanostructured lipid carrier, Stress, TNF-alpha

Persistent inflammation is a fundamental biological reaction triggered by harmful stimuli such as infectious agents, injured cells, stress exposures, or irritating substances[1,2]. If unresolved, excessive inflammation may contribute to the pathogenesis of disease, aggravating severity and hindering the progression of both physical and psychological symptoms. However, the optimal therapeutic treatments for inflammation-induced conditions still require investigation.

Especially the hippocampus plays a critical role in emotional regulation, memory formation, and stress response. As a key structure involved in learning and behavior, it modulates the hypothalamic-pituitary-adrenal

[1]Chulabhorn International College of Medicine, Thammasat University, Pathumthani 10120, Thailand. [2]Department of Basic Medical Sciences, Faculty of Medicine, Siam University, Bangkok 10160, Thailand. [3]National Nanotechnology Centre, National Science and Technology Development Agency, Pathumthani 12120, Thailand. [4]Center for Research Innovation and Biomedical Informatics, Faculty of Medical Technology, Mahidol University, Nakhon Pathom 73170, Thailand. [5]Department of Anatomy, Faculty of Medical Science, Naresuan University, Phitsanulok 65000, Thailand. [6]Faculty of Medicine, Praboromarajchanok Institute, Ministry of Public Health, Nonthaburi 11000, Thailand. ✉email: mattaka@nanotec.or.th

(HPA) axis, which governs stress regulation. Chronic stress and neuroinflammation, often implicated in the pathophysiology of behavioral disorders, can significantly disrupt hippocampal function[3,4]. Neuroinflammation, characterized by the activation of glial cells (e.g. microglia and astrocytes), is a prominent feature of psychiatric and neurodegenerative diseases. Inflammatory cytokines, such as interleukin-1 (IL-1), interleukin-6 (IL-6), interferon-gamma (IFN-γ), and tumor necrosis factor-alpha (TNF-alpha), are upregulated in response to neuroinflammation and can exert direct harmful effects on hippocampal neurons by disrupting synaptic plasticity, impairing neurogenesis, and promoting neuronal apoptosis[5–7]. This leads to hippocampal dysfunction, which is closely associated with the onset of behavioral abnormalities, mood disorders (e.g., anxiety, depression), and cognitive impairments. Chronic neuroinflammation disrupts the immune response in the brain, intensifying hippocampal damage and altering key neurotransmitter systems, such as monoamines and glutamate, which are essential for mood regulation and cognitive function[8–10]. Additionally, neuroinflammation could induce oxidative stress, generating reactive oxygen species (ROS) that contribute to neuronal damage and hinder neuroplasticity in the hippocampus[11,12]. This cascade of events disrupts cognitive and emotional processes, forming the basis of the pathophysiology of sickness-like symptoms and stress-related behavioral disorders[13]. Targeting neuroinflammation in the hippocampus, therefore, represents a promising therapeutic strategy.

Traditional management of neuroinflammatory conditions has heavily relied on anti-inflammatory medications such as aspirin, ibuprofen, diclofenac, betamethasone, and dexamethasone (DEXA). While these drugs can effectively alleviate inflammation stage-like symptoms, their prolonged use often leads to significant adverse effects, including gastrointestinal, cardiovascular, and renal problems and increased susceptibility to infections[14–16]. These side effects indicate the need for safer and more effective alternatives to current anti-inflammatory treatments. While current medications provide symptomatic relief, some treatments fail to address the long-term impacts of neuroinflammatory processes.

Among natural herbs, andrographolide (Andro), a diterpenoid lactone derived from *Andrographis paniculata*, is a promising alternative candidate due to its beneficial effects. Several studies have revealed Andro's anti-inflammatory and immunomodulatory effects[17]. Andro has demonstrated effectiveness in suppressing cytokines production and alleviating neurodegenerative-related diseases[18]. Andro is a promising candidate as a therapeutic agent for inflammation, reducing disruption of blood-brain barrier (BBB) permeability in subarachnoid hemorrhage, mitigating neuronal cell injury, and promoting neurogenesis[19,20]. However, the therapeutic application of Andro is limited by its poor bioavailability, pH intolerance, and rapid degradation, which diminish its efficacy. Addressing these concerns necessitates the development of innovative delivery systems to enhance the stability and oral efficacy of Andro, thereby maximizing its pharmacotherapeutic potential.

Facilitating enhanced drug delivery methods, especially nanostructured lipid carriers (NLCs), provides highly effective platforms, particularly for compounds, e.g., cannabidiol or Andro that have low solubility and stability[21–24]. NLCs encapsulate bioactive compounds, preventing degradation and enabling controlled release. This encapsulation can boost drug bioavailability and improve therapeutic outcomes while reducing systemic toxicity. The development of AndroNLCs formulations shows promise in enhancing the efficacy of central nervous system drug delivery, offering a targeted strategy as supported by recent studies[23,25].

Therefore, this study aimed to enhance Andro's delivery and therapeutic potential while addressing the limitations of current treatments. Specifically, the main objectives were to develop a novel, safe AndroNLC formulation that improves stability and oral efficacy, as demonstrated by in vitro anti-inflammatory activity. Additionally, this study sought to evaluate the therapeutic outcomes of AndroNLCs in mitigating neuroinflammation and associated behavioral changes in animal models with induced systemic inflammation, comparing these results to those of traditional anti-inflammatory and anti-stress medications. It was hypothesized that AndroNLCs could potentially translate into an effective treatment for inflammation-related mental illness.

Results

Physicochemical properties and characteristics of AndroNLCs

Blank and AndroNLCs were formulated by high-pressure homogenization at high temperature. The particle size, polydispersity index (PdI) and zeta potential were evaluated by dynamic light scattering (DLS). The diameter of Blank and AndroNLCs was 125.40 ± 0.90 nm and 131.40 ± 1.30 nm. Additionally, the PdI value of formulations was 0.17 ± 0.02, indicating homogenous size distributions. Moreover, the zeta potential of these nanoparticles was − 25.11 ± 0.39 mV and − 33.33 ± 1.03 mV, respectively. These results suggested that AndroNLCs demonstrate good colloidal stability. Furthermore, the percent encapsulation efficiency (%EE) of Andro in the NLCs was calculated and found at 89.11 ± 0.15%, indicating efficient loading of the active compound into the NLCs. These results demonstrated that AndroNLCs are a promising delivery system for Andro, with advantages in controlling particle size, ensuring stability, and maximizing encapsulation efficiency. In addition, the transmission electron microscopy (TEM) analysis results showed that both Blank and AndroNLCs had uniformly spherical and well-dispersed characteristics (Fig. 1A).

Over three months, the stability and characteristics of both Blank and AndroNLCs were evaluated to determine their potential for sustained application (Fig. 1B,C). The Blank had a size of 125.40±0.90 nm, with a PdI of 0.18 ± 0.01 and a zeta potential of − 25.11 ± 0.39 mV. Throughout the study, by the third month, the size of the Blank gradually increased, ultimately reaching 140.33 ± 0.93 nm. This increase suggests a tendency towards instability. Additionally, the PdI increased slightly from 0.18 ± 0.01 to 0.20 ± 0.03, indicating a broader size distribution and reduced uniformity. Despite these changes, the zeta potential of the Blank remained relatively stable, fluctuating around − 24.85 ± 2.20 mV, which implies that electrostatic repulsion continues to effectively maintain particles. While, the AndroNLCs began with a size of 131.40 ± 2.50 nm and a PdI of 0.17 ± 0.02. Over the three-month period, their size slightly increased to 139.99 ± 0.44 nm, indicating the degree of aggregation, but this increase was less pronounced than the Blank. The PdI improved, decreasing from 0.17 ± 0.02 to

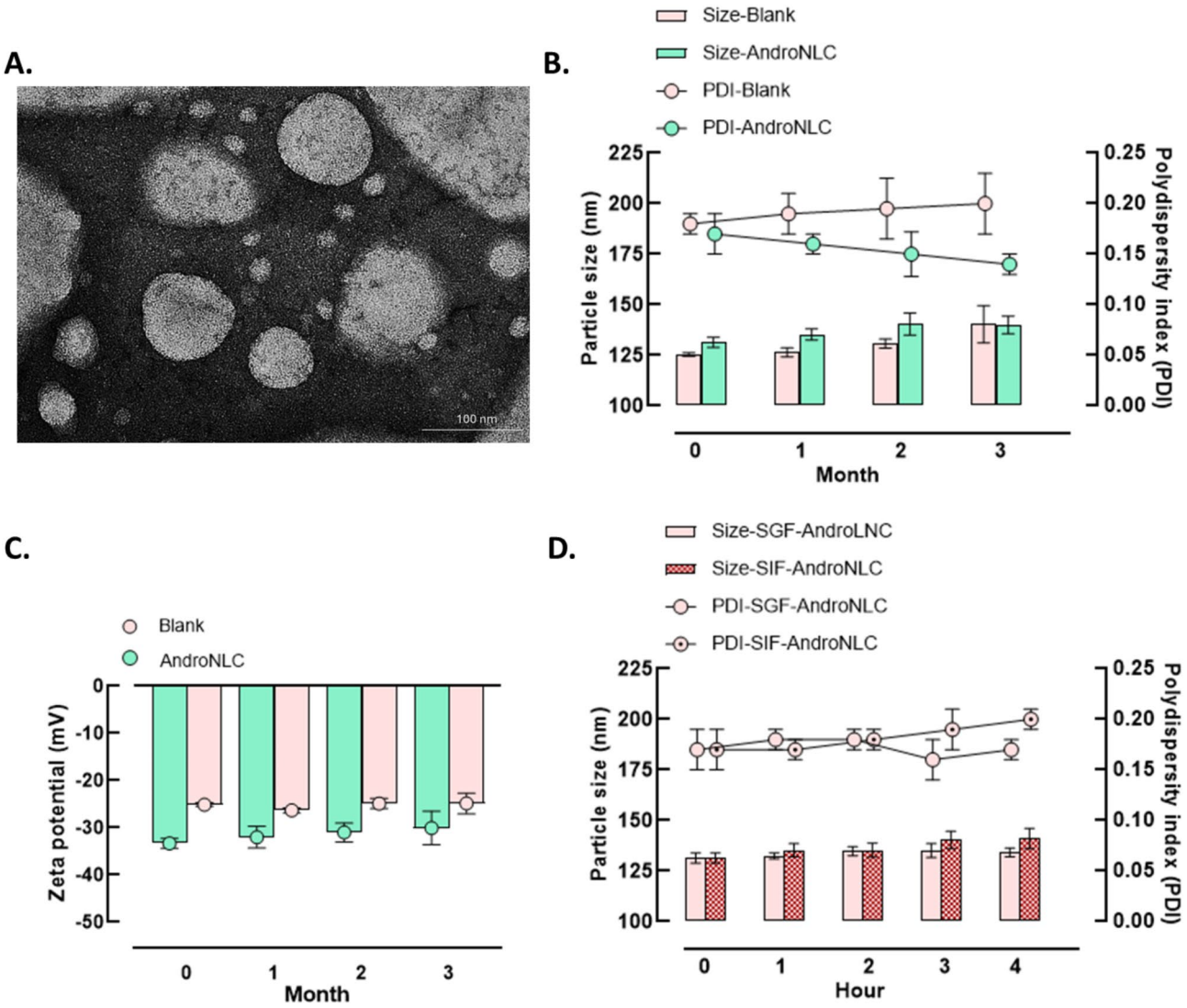

Fig. 1. Physicochemical characterization of andrographolide-loaded nanostructured lipid carriers (AndroNLCs). (**A**) Transmission electron micrograph of AndroNLCs, (**B**) the stability of Blank and AndroNLCs during 3 months of storage in distilled water at 25 °C, particle size and polydispersity index (PDI), (**C**) the zeta potential, and (**D**) the stability of AndroNLCs during 4 h of treatment in simulated gastric fluid (SGF) and simulated intestinal fluid (SIF) at 37 °C. PdI was measured in distilled water.

0.14 ± 0.01, which reflects a more uniform size distribution and enhanced stability over time. The zeta potential of AndroNLCs started at − 33.33 ± 1.03 mV and slightly reduced to − 30.05 ± 3.56 mV by the end of the 3-month study. Although there was a reduction, the zeta potential remained significantly negative, indicating continued electrostatic stability and effective resistance to aggregation, which confirms the stability of the formulation.

Stability of AndroNLCs for oral efficacy in simulated gastric and intestinal conditions

The stability of AndroNLCs was assessed in the simulated gastric fluid (SGF) and simulated intestinal fluid (SIF) conditions to evaluate the robustness in physiological environments (Fig. 1D). At the beginning, AndroNLCs had a particle size of 131.40 ± 2.50 nm with a PdI of 0.17 ± 0.02. Throughout the incubation in SGF, the particle size showed only a slight increase, ending at 134.18 ± 2.17 nm. The PdI remained relatively stable, with minor fluctuations around 0.17–0.18. This stability in size and distribution suggests that AndroNLCs are stable in acidic environments, resist the enzymatic activity of pepsin, and maintain structural integrity while present in the stomach. After SIF exposure, the particle size had a slight increase to 141.10 ± 5.00 nm. The PdI showed minimal changes, ranging from 0.17 to 0.20. These results indicate that AndroNLCs maintain size distribution and structural stability even in the presence of pancreatin and bile salts, which mimic the enzymatic and bile conditions in the intestinal lumen. These results show that the highly negative zeta potential of AndroNLCs contributes to electrostatic stability, preventing aggregation and maintaining uniform dispersion in both SGF and SIF studies.

Cytotoxicity and anti-inflammatory profiles of AndroLNCs in an in vitro study

The cytotoxicity of Blank, Andro, and AndroNLCs was assessed in SH-SY5Y human neuroblastoma cell lines across different concentrations. At lower concentrations (0.00 to 15.60 ppm), all treatments demonstrated relatively high cell viability, exceeding 80%. However, as the concentration increased, there was a decline in viability, particularly for the Blank and Andro. For instance, at a concentration of 31.00 ppm, cell viability dropped to 58.37 ± 6.14% for Blank and 64.08 ± 2.02% for Andro, while AndroNLCs maintained a relatively higher viability of 56.48 ± 2.19%. This trend continued at higher concentrations, with significant reductions in cell viability, Blank dropped to 25.67 ± 1.50%, Andro to 41.25 ± 5.95%, and AndroNLCs to 52.33 ± 5.39% at the highest concentration of 250 ppm. Notably, the AndroNLCs consistently displayed better efficacy than the Blank and Andro groups, with a less pronounced decline in viability as concentration increased (Fig. 2A). This result suggests that AndroNLCs exhibit reduced cytotoxicity. Concentrations between 7.81 and 15.60 ppm of AndroNLCs enhanced cell viability, suggesting that 10 ppm or 10 mg/kg might be a promising and safe dose for animal studies. For these studies, dosages up to 10 times the safety dose, approximately 1.0 ppm or 10 mg/kg, can be considered.

The inflammation profiles in SH-SY5Y neuronal culture cells pre-treated with lipopolysaccharide (LPS) for 24 h were assessed by measuring IL-6 and TNF-alpha levels (Fig. 2B,C). In the control group, IL-6 levels remained very low, at 2.94 ± 0.24 pg/mL, indicating minimal inflammation in untreated cells. LPS treatment alone (vehicle) led to a dramatic increase in IL-6 levels, averaging 327.00 ± 5.29 pg/mL compared to controls [$F(5,12) = 1877$; $P < 0.001$], reflecting a strong inflammatory response. When treated with 2.5 µg/mL Andro, IL-6 levels slightly decreased to 316.10 ± 1.41 pg/mL, suggesting a modest anti-inflammatory effect. Increasing the concentration to 5 µg/mL Andro significantly reduced to 278.50 ± 4.93 pg/mL [$F(4,10) = 1025$; $P < 0.001$], indicating a dose-dependent effect. However, when cells were treated with AndroNLCs, the anti-inflammatory response was more pronounced. At 2.5 µg/mL AndroNLC, IL-6 levels significantly dropped to 136.30 ± 1.78 pg/mL, and at 5 µg/mL AndroNLC, levels further decreased to 91.37 ± 0.37 pg/mL [$F(4,10) = 1025$; $P < 0.001$], demonstrating the most potent anti-inflammatory effect. Similarly, TNF-alpha levels in the control group were low, at 19.69 ± 0.00 pg/mL. LPS treatment significantly increased to 44.69 ± 0.00 pg/mL in the vehicle group [$F(5,12) = 1797$; $P < 0.001$]. Treatment with 2.5 µg/mL Andro significantly reduced TNF-alpha levels to 24.17 ± 0.28 pg/mL, with further reduction observed at 5 µg/mL Andro, where levels were 22.60 ± 0.45 pg/mL [$F(4,10) = 1750$; $P < 0.001$]. AndroNLCs had a more potent anti-inflammatory effect. At 2.5 µg/mL AndroNLCs, TNF-alpha levels to 18.65 ± 0.21 pg/mL, and at 5 µg/mL AndroNLC, levels were the lowest, at 18.54 ± 0.10 pg/mL [$F(4,10) = 1759$; $P < 0.001$].

These results suggest that LPS treatment caused a substantial inflammatory response, as indicated by elevated IL-6 and TNF-alpha levels. Andro demonstrated a dose-dependent anti-inflammatory effect, with higher concentrations leading to greater reductions in both IL-6 and TNF-alpha levels. Interestingly, AndroNLCs could be more effective in mitigating LPS-induced inflammation in SH-SY5Y neuronal culture cells than natural Andro form.

Physical and biochemical responses of AndroNLCs in mice with TNF-alpha induced neuroinflammation

According to the experiment in the animal study, as shown in Fig. 3A, no differences in the starting body weight of the mice were observed among the groups (Fig. 3B). Vehicle-treated mice with TNF-alpha-induced inflammation had a lower final body weight [$F(5,48) = 5.462$; $P < 0.001$] and a reduced percentage of daily body weight change compared to the controls [$F(5,48) = 7.339$; $P < 0.001$]. However, after a 14-day treatment, Andro, AndroNLCs, DEXA (dexamethasone) and venlafaxine (VLX) significantly restored final body weight [$F(4,40) = 6.153$; $P < 0.001$] and percentage change in daily body weight gain compared vehicle-treated mice with TNF-alpha-induced inflammation [$F(4,40) = 8.771$; $P < 0.001$], as presented in Fig. 3C,D. Furthermore, repeated peripheral TNF-alpha-induced inflammation had a compensatory effect on target organs in neuroimmunological and stress responses, as indicated by the increased relative wet weights of the adrenal glands [$F(5,48) = 6.714$; $P < 0.001$], spleen [$F(5,48) = 5.768$; $P < 0.001$], and thymus to body weight ratio[$F(5,48) = 5.619$; $P < 0.001$]. All interventions were significantly effective in in restoring the increased organ weights [adrenal glands: $F(4,40) = 8.549$ $P < 0.001$, spleen: [$F(4,40) = 6.519$; $P < 0.001$], thymus: [$F(4,40) = 6.461$; $P < 0.001$] associated with the detrimental effects of inflammatory induction (Fig. 3E–G).

At the biochemical level, vehicle-treated mice with TNF-alpha-induced inflammation showed markedly increased serum corticosterone (CORT, $F(5,48) = 4.218$; $P = 0.003$), alanine transaminase (ALT, $F(5,48) = 4.218$; $P = 0.003$ $P < 0.001$) and (J) aspartate aminotransferase (AST, $F(5,48) = 4.218$; $P = 0.003$; $P < 0.001$] and hippocampal IL-6 [$F(5,24) = 17.210$; $P < 0.001$] and TNF-alpha [$F(5,24) = 11.70$; $P < 0.001$], as well as malondialdehyde (MDA, $F(5,24) = 4.218$; $P = 0.003$ $P < 0.001$) levels compared to the controls (Fig. 3H–M). The analysis of MDA levels as a marker of oxidative stress in hippocampal tissue revealed a significant increase in the vehicle-treated group. Treatment with AndroNLCs effectively reduced MDA levels, showing comparable effects to DEXA and superior efficacy to Andro alone. These findings indicate that AndroNLCs can effectively mitigate oxidative stress-indeced by TNF-alpha (Fig. 3M). Together, these results indicate that inflammation leads to significant biochemical dysregulation, reflecting systemic stress, hepatic injury, and neuroinflammatory responses.

Among these interventions, AndroNLCs and DEXA showed higher efficacy in reducing serum CORT [$F(4,40) = 3.599$; $P = 0.014$] and AST [$F(4,40) = 3.599$; $P = 0.014$] (Fig. 3H and J). AndroNLCs also significantly lowered hippocampal IL-6 levels [$F(4,20) = 9.127$; $P < 0.001$], while both Andro and AndroNLCs reduced TNF-alpha levels ($P = 0.010$) (Fig. 3J). Therefore, AndroNLCs potentially alleviated stress and inflammatory markers.

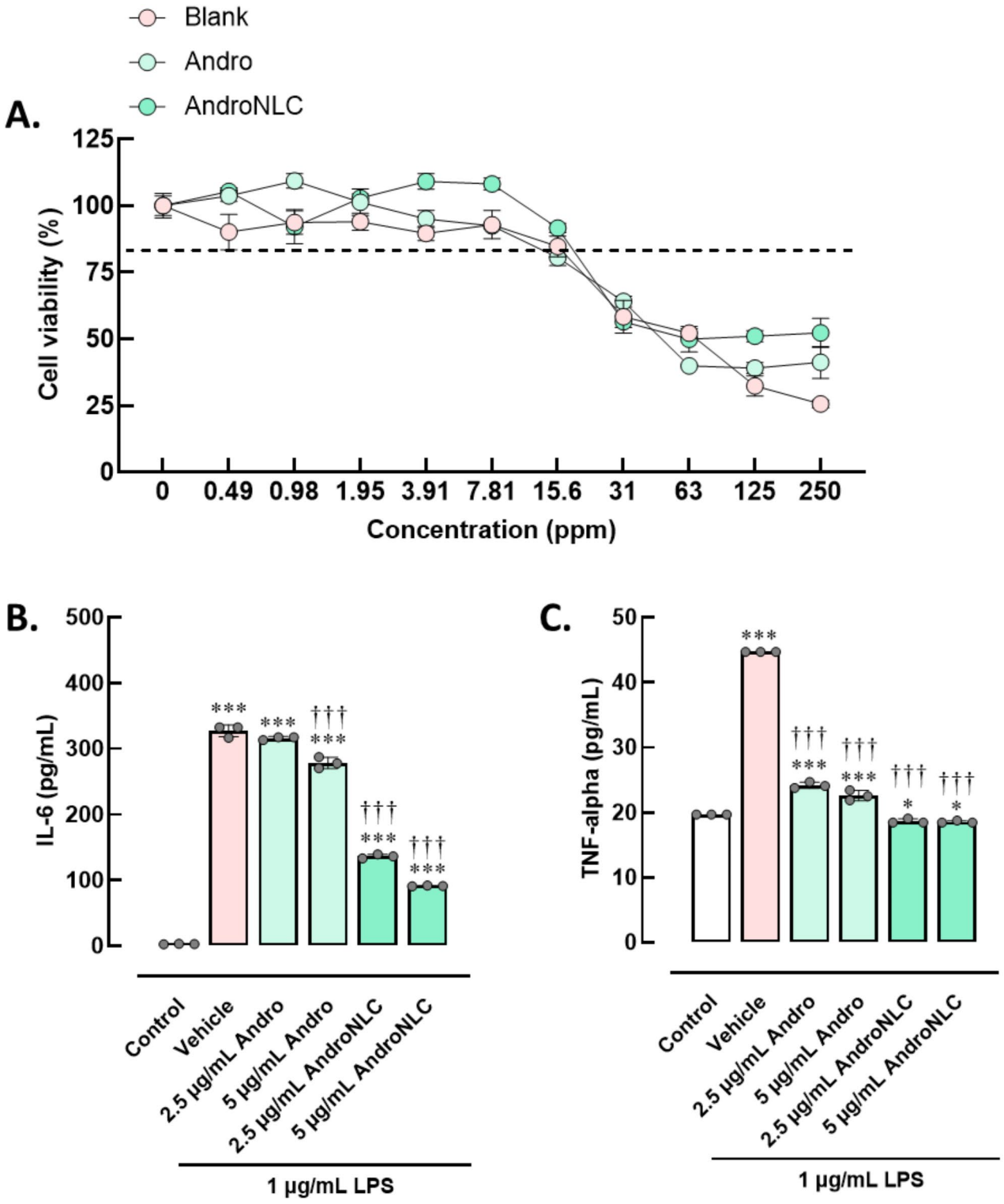

Fig. 2. Safety and anti-inflammatory profiles in an in vitro study of Blank, natural Andrographolide (Andro), and Andrographolide-loaded nanostructured lipid carriers (AndroNLCs). (**A**) The percentages of cell viability in the cytotoxicity test, (**B**) changes in pro-inflammatory levels of IL-6, and (**C**) TNF-alpha in SH-SY5Y neuronal cultures exposed to lipopolysaccharides (LPS). The data are presented as mean ± SEM ($n = 3$ per group). $^{*}P < 0.05$, $^{***}P < 0.001$ versus control, $^{\dagger\dagger\dagger}P < 0.001$ versus vehicle.

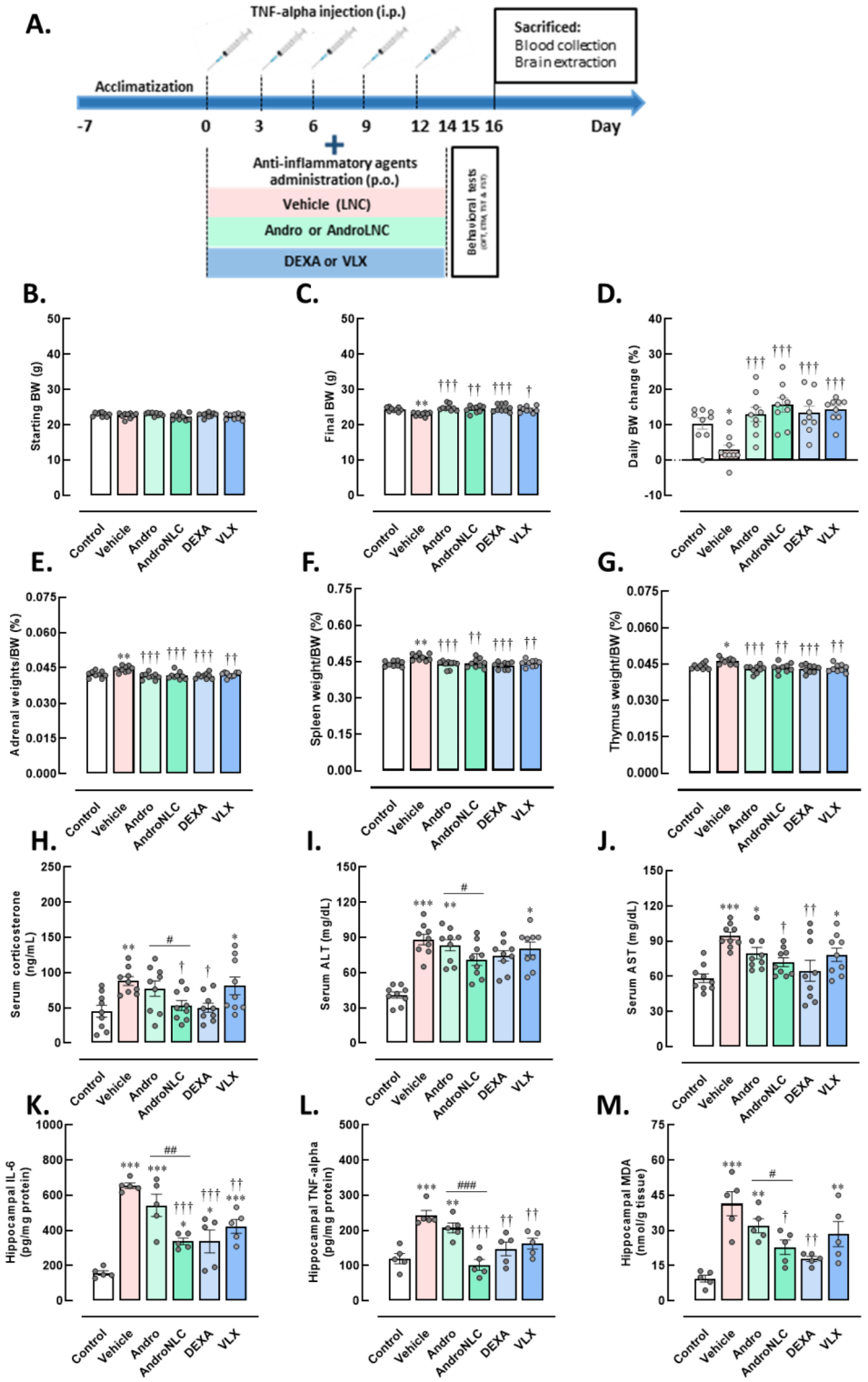

Fig. 3. Physical and biochemical profiles of body and organ weights, serum and hippocampal biomarkers in male mice with TNF-alpha-induced inflammation. (**A**) Experimental design in the animal study, (**B**) starting body weight, (**C**) final body weight, (**D**) percentage of daily weight gain change, (**E**) relative adrenal gland weight, (**F**) spleen weight, (**G**) thymus weight, (**H**) serum corticosterone, (**I**) alanine transaminase (ALT) and (**J**) aspartate aminotransferase (AST) levels, (**K**) hippocampal interleukin (IL)-6, (**L**) tumor necrosis factor (TNF)-alpha and (**M**) malondialdehyde (MDA) levels. The data are presented as mean ± SEM ($n = 5$–9 mice per group). $^{*}P < 0.05$, $^{**}P < 0.01$, $^{***}P < 0.001$ versus control, $^{\dagger}P < 0.05$,$^{\dagger\dagger}P < 0.01$, $^{\dagger\dagger\dagger}P < 0.001$ versus vehicle, and $^{\#}P < 0.05$, $^{\#\#}P < 0.01$,$^{\#\#\#}P < 0.001$ versus Andro. Andro, Andrographolide; AndroNLCs, Andrographolide-loaded nanostructured lipid carriers; DEXA, dexamethasone; VLX, venlafaxine.

Although VLX is known for its antidepressant and anti-neuroinflammatory effects, it did not directly attenuate inflammation-induced stress, liver toxicity, or oxidative stress in these male mice, as indicated by sustained increases in serum CORT, ALT, AST, and hippocampal levels of IL-6, TNF-alpha, and MDA (Fig. 3H–M).

These physical and biochemical results suggest that AndroNLCs could be considered an alternative option for conditions associated with stress and inflammation, potentially offering a beneficial alternative to traditional anti-inflammatory treatments while attenuating Andro toxicity through the NLC formulation. As, mice with TNF-alpha-induced inflammation exhibited elevated serum ALT and AST levels compared to the control group. Treatment with AndroNLCs significantly reduced these levels, demonstrating effects comparable to DEXA and greater efficacy than Andro alone. These findings indicate that AndroNLCs may help mitigate liver injury in mice.

Behavioral responses of AndroNLCs in mice with TNF-alpha induced neuroinflammation

Regarding behavioral alterations, vehicle-treated mice with TNF-alpha-induced inflammation exhibited significant changes, including increased hyperlocomotor activity, heightened emotionality, generalized anxiety, and depressive-like behaviors. Vehicle-treated group had less time spent in the inner zone of the arena [$F(5,48) = 3.660$; $P = 0.007$] and showed an increased number of crossed lines [$F(5,48) = 3.526$; $P = 0.009$] and rearings [$F(5,48) = 3.652$; $P = 0.007$] in the open field test (OFT) (Fig. 4A–C). No difference in baseline latency was observed in the inhibitory avoidance test (Fig. 4D). Vehicle-treated group Vehicle-treated mice with TNF-alpha-induced inflammation exhibited conditioned learned fear as indicated by prolonged inhibitory avoidance latency [trail I: $F(5,48) = 5.175$; $P < 0.001$ and trail II: $F(5,48) = 8.085$; $P < 0.001$] (Fig. 4E-F) but did not show a change in the time spent in the one-way escape test in the elevated T-maze (ETM) (Fig. 4G). Furthermore, a significant increase in immobility time was observed in the TST [$F(5,48) = 3.127$; $P = 0.016$], with increased immobility in the FST [$F(5,48) = 3.932$; $P = 0.005$] in vehicle-treated groups compared to controls (Fig. 4H–I).

Conversely, the administration of these interventions effectively alleviated the behavioral abnormalities. Andro, AndroNLCs, and DEXA increased the time spent in the inner zone during the OFT [$F(4,40) = 4.706$; $P = 0.003$], and all treatments restored the total number of line crossings [$F(4,40) = 4.034$; $P = 0.008$]. However, Andro, AndroNLCs, and VLX could restore the number of rearings [$F(4,40) = 4.050$; $P = 0.008$], but DEXA did not (Fig. 4A–C). In the ETM test, VLX-treated mice with TNF-alpha-induced inflammation spent more time in the enclosed arm during inhibitory avoidance trial I [$F(4,40) = 2.687$; $P = 0.045$) (Fig. 4E). Interestingly, all these interventions reduced conditioned fear in mice with TNF-alpha-induced inflammation, as observed by decreased avoidance in trial II [$F(4,40) = 5.759$; $P < 0.001$] (Fig. 4F). In addition, AndroNLCs, DEXA, and VLX-treated mice with TNF-alpha-induced inflammation showed a significant increase in the time spent in the open arm of the one-way escape test [$F(4,40) = 6.413$; $P = 0.004$] (Fig. 4G), suggesting that these treatments had potential panicolytic effects.

Besides anxiety evaluation in mice with TNF-alpha-induced inflammation, the results from depression tests found that AndroNLCs significantly alleviated depression-like behaviors, similar to DEXA and VLX in the tail suspension test (TST) [$F(4,40) = 3.425$; $P = 0.017$] and to Andro and VLX in the forced swim test (FST) [$F(4,40) = 5.265$; $P = 0.002$], when compared to the vehicle-treated group (Fig. 4H–I). Notably, AndroNLCs showed superior efficacy compared to Andro in alleviating panic-like behavior in the one-way escape test of the ETM [$t(16) = 2.477$; $P = 0.012$) and exhibited antidepressant effects in the TST [$t(16) = 1.786$; $P = 0.047$] (Fig. 4G–H).

To sum up, these findings suggest that AndroNLCs could offer both anxiolytic and antidepressant-like effects, showing promise as a therapeutic intervention for alleviating behavioral abnormalities linked to inflammation-induced anxiety-, panic-, and depression-like behaviors. AndroNLCs could surpass the efficacy of Andro alone and align with standard treatments, including anti-inflammatory and anti-stress agents.

Histological changes in hippocampal neurons in mice with TNF-alpha-induced neuroinflammation

Morphological changes in hippocampal neurons were observed using H&E staining (Fig. 5). The hippocampus consists of interlocking grey matter structures, including the cornu ammonis (CA) and the dentate gyrus (DG), separated by the hippocampal sulcus. The CA is divided into CA1, CA2, CA3, and CA4 regions, with the DG covering CA4 (Fig. 5.1A–6A). In the control group, pyramidal neurons had rounded nuclei with intact nucleoli and a border of cytoplasm, with closely packed cell bodies (red arrow) arranged in 3 to 4 rows in the pyramidal cell layer (PCL) of the CA1 to CA4 regions (Fig. 5.1B–1E). The granule cell layer (GCL) in the DG typically presents a rounded to oval-shaped aggregation of granule cell bodies (Fig. 5.1F). Vehicle-treated mice with TNF-alpha-induced inflammation showed signs of cell death, with nuclei becoming condensed and dark, and cell bodies appearing dark, shrunken, and loosely packed (black arrow), as well as dark, shrunken granule cell bodies in the hippocampal subregion (Fig. 5.2B–2F). Treatment with Andro, AndroNLCs, or DEXA reduced histopathological damage in the CA1 to CA4 and DG regions, displaying more regularly arranged pyramidal and granule cell bodies, with a few shrunken and deeply stained pyknotic nuclei (Fig. 5.3B–3F, 5.4B–4F, and 5.5B–5F). However, treatment with VLX in CA3, CA4, and DG showed shrunken, dark-stained nuclei, often referred to as dark neurons, indicating degenerating or dying neurons (Fig. 5.6D–6F).

Since the DG is a key hub for integrating neurobiological processes that regulate emotional and behavior expression, making it an exciting target for research and therapeutic interventions in mood disorders. Quantitative histological DG analysis revealed that vehicle-treated mice with TNF-alpha-induced inflammation had an increased number of pyknotic cells [$F(5,42) = 55.34$; $P < 0.001$] and reduced the PCL and GCL thickness [$F(5,84) = 59.11$; $P < 0.001$] and fewer surviving cells compared to the control group [$F(5,42) = 2.408$; $P < 0.001$]. Treatment with Andro and AndroNLCs resulted in a reduction in pyknotic cells [$F(4,35) = 55.52$; $P < 0.001$] and

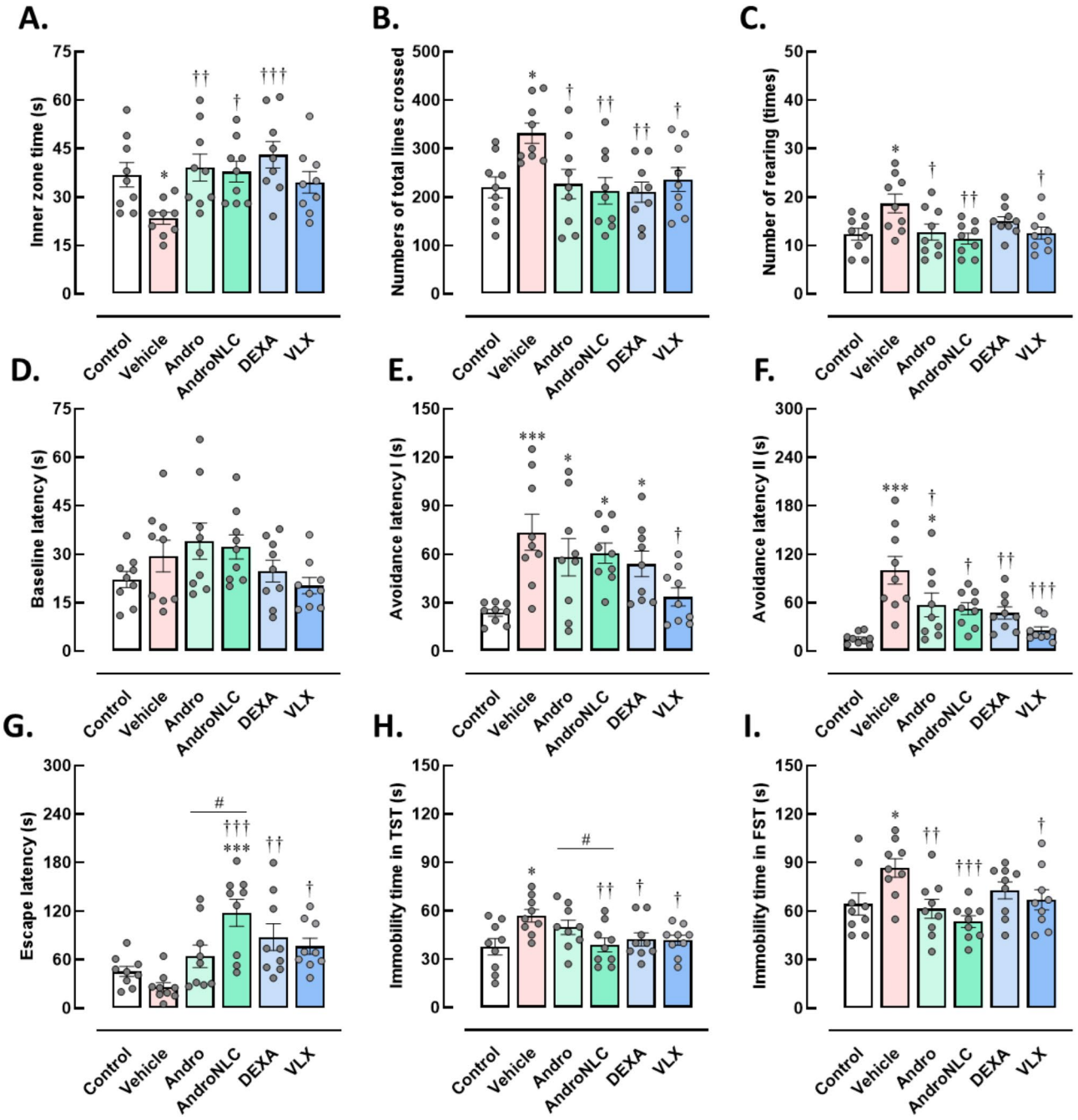

Fig. 4. Behavioral profiles of locomotor activity and anxiety- and depression-like behaviors in male mice with TNF-alpha-induced inflammation using the open-field test (OFT), elevated T-maze (ETM), tail suspension test (TST), and forced swimming test (FST). (**A**) Time spent in the inner zone, (**B**) total number of line crosses, (**C**) number of rearing activity in the open arena, (**D**) time spent in inhibitory avoidance trials at baseline, (**E**) trail 1, (**F**) trail 2, (**G**) time spent in the one-way escape latency test of the ETM, (**H**) immobility time in the TST and (**I**) in the FST. The data are presented as mean ± SEM ($n = 9$ mice per group). $^{*}P < 0.05$, $^{***}P < 0.001$ versus control, $^{\dagger}P < 0.05$, $^{\dagger\dagger}P < 0.01$, $^{\dagger\dagger\dagger}P < 0.001$ versus vehicle and $^{\#}P < 0.05$ versus Andro. Andro, Andrographolide; AndroNLCs, Andrographolide-loaded nanostructured lipid carriers; DEXA, dexamethasone; VLX, venlafaxine.

restored the thickness of the PCL and GCL [$F(4,70) = 37.970$; $P < 0.001$], as well as the number of surviving cells [$F(4,35) = 15.97$; $P < 0.001$], compared to vehicle (Table 1).

Specifically, AndroNLCs have a superior neuroprotective effect against inflammatory induction by TNF-alpha compared to Andro alone, as demonstrated by a significantly higher number of surviving cells in the hippocampal CA1 [$t(14) = 2.711$; $P = 0.017$] to CA2 regions [$t(14) = 2.667$; $P = 0.018$]. These results indicate that

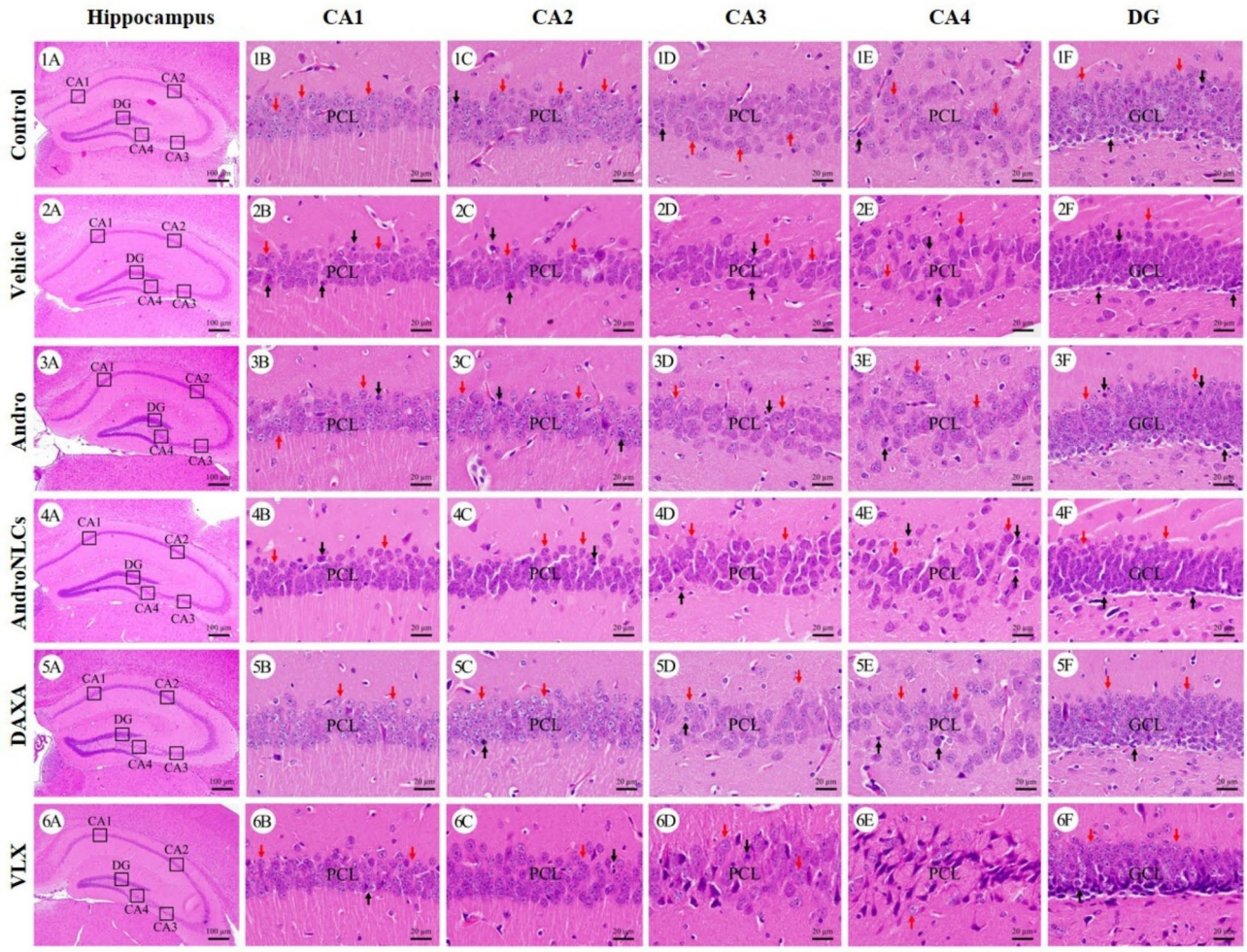

Fig. 5. Histological profiles of H&E-stained hippocampal subregion sections, including cornu ammonis (CA) areas CA1, CA2, CA3, CA4, and the dentate gyrus (DG) in male mice with TNF-alpha-induced inflammation. Control mice (1 A–1 F); Vehicle-treated inflamed mice (2 A–2 F); Andro-treated inflamed mice (3 A–3 F); AndroNLCs-treated inflamed mice (4 A–3 F); DEXA-treated inflamed mice (5 A–5 F); VLX-treated inflamed mice (6 A–6 F). Red arrows indicate normal neuron cells, and black arrows indicate pyknotic neuronal cells. Scale bars represent 50 µm (magnification, 40×). Andro, Andrographolide; AndroNLCs, Andrographolide-loaded nanostructured lipid carriers; DEXA, dexamethasone; PCL, pyramidal cell layer; GCL, granule cell layer; VLX, venlafaxine.

AndroNLCs effectively facilitate the attenuation of hippocampal neural damage in inflamed mice, demonstrating efficacy comparable to traditional treatments (i.e., DEXA and VLX).

Discussion

Inflammation, driven by the production of cytokines, chemokines, and reactive oxygen species, significantly affects both behavior and biochemistry, creating a complex interplay between the immune system and the nervous system[1,5,6]. While anti-inflammatory medications can manage inflammation, long-term side effects and delayed responses can occur[14–16]. Therefore, finding natural alternatives remains a necessary challenge.

This study has developed Andro delivery using NLCs, an anti-inflammatory and immunomodulating formulation of Andro, which addresses its limited physicochemical properties and pharmacology. The formulation demonstrates significant advancements in therapeutic utility, achieving homogeneity and stability with a particle size of 131.40 ± 1.30 nm, a PdI of 0.17 ± 0.02, and a zeta potential of − 33.33 ± 1.03 mV, indicating a consistent and uniform distribution of AndroNLCs. Based on these findings, the potential of NLCs as an effective delivery system for Andro has been reported[26]. The slightly larger size of AndroNLCs compared to the Blank formulation (131.40 nm vs. 125.40 nm) is within a reasonable range for NLCs, ensuring suitability for drug delivery applications. The size distribution, indicated by the PdI, describes the width of the particle size distribution. A PdI value ranging from 0.1 to 0.25 suggests a narrow size distribution. Here, the low PdI (0.17–0.18) indicates uniform particle size distribution, which is essential for consistent drug release kinetics and therapeutic efficacy, including antimicrobial effects and crossing the BBB[27]. Additionally, the more negative

Parameters	Treatment group					
	Control	Vehicle	Andro	AndroNLCs	DEXA	VLX
Thickness of pyramidal layer (μm)						
CA1	37.45 ± 0.59	32.15 ± 0.67**	36.31 ± 0.83†	36.57 ± 0.74†	38.37 ± 0.77††	38.26 ± 1.47††
CA2	43.45 ± 1.01	29.54 ± 0.66**	40.19 ± 0.82††	36.22 ± 0.75*$^{\dagger\dagger\#\#}$	40.44 ± 1.47††	44.25 ± 1.36††
CA3	57.65 ± 1.76	28.31 ± 1.08**	44.18 ± 1.18**††	40.52 ± 1.42**††	44.20 ± 0.96**††	54.51 ± 1.04††
CA4	74.19 ± 3.69	42.20 ± 1.54**	55.39 ± 1.56**††	58.15 ± 1.81**††	64.68 ± 1.67*††	49.38 ± 1.48**
DG	70.41 ± 1.63	44.44 ± 0.86**	61.36 ± 0.98**††	49.77 ± 0.92**$^{\dagger\dagger\#\#}$	55.84 ± 1.18**††	46.63 ± 0.99**
Number of surviving cells (cells/field)						
CA1	90.63 ± 1.58	74.00 ± 2.55**	82.88 ± 1.47†	90.50 ± 2.40$^{\dagger\dagger\#}$	88.00 ± 0.98††	80.75 ± 1.97**†
CA2	117.25 ± 1.41	101.38 ± 1.94**	111.75 ± 1.03†	118.00 ± 2.10$^{\dagger\dagger\#}$	116.13 ± 1.51††	114.00 ± 4.14††
CA3	80.63 ± 2.34	61.00 ± 0.63**	73.00 ± 1.80††	76.63 ± 1.18††	66.38 ± 1.34**†	76.50 ± 4.15††
CA4	81.75 ± 3.81	68.13 ± 0.93**	78.88 ± 0.85††	79.25 ± 0.94††	79.63 ± 3.82††	75.63 ± 3.36†
DG	140.25 ± 1.68	122.38 ± 1.00**	146.63 ± 2.99††	139.13 ± 1.17$^{\dagger\dagger\#}$	140.50 ± 1.20††	133.38 ± 3.66†
Number of pyknotic cells (cells/field)						
CA1	1.13 ± 0.30	3.63 ± 0.42**	1.63 ± 0.38††	2.13 ± 0.23†	1.25 ± 0.16††	2.38 ± 0.26†
CA2	2.13 ± 0.30	6.13 ± 0.40**	2.75 ± 0.45††	2.63 ± 0.26††	2.50 ± 0.27††	2.50 ± 0.19††
CA3	1.75 ± 0.25	7.25 ± 0.49**	2.25 ± 0.25††	1.88 ± 0.30††	2.75 ± 0.25††	2.88 ± 0.23††
CA4	2.25 ± 0.45	10.00 ± 0.78**	3.38 ± 0.38††	3.13 ± 0.30††	4.25 ± 0.37*††	3.88 ± 0.40††
DG	2.88 ± 0.35	12.25 ± 0.67**	4.25 ± 0.56††	3.63 ± 0.38††	4.38 ± 0.32††	4.13 ± 0.44††

Table 1. Pyramidal cell layer, number of surviving cells and pyknotic cells in the hippocampus (CA1, CA2, CA3, and CA4), and granular cell layer in the dentate gyrus (DG) after 14 days of vehicle, Andrographolide (Andro), Andrographolide-nanostructured lipid carriers (AndroNLCs), dexamethasone (DEXA) or Venlafaxine (VLX) treatments in mice with neuroinflammation. The data are presented as mean ± SEM ($n = 4$ mice per group). *$P < 0.05$, **$P < 0.01$ versus control, $^{\dagger}P < 0.05$, $^{\dagger\dagger}P < 0.01$, versus vehicle, $^{\#}P < 0.05$, $^{\#\#}P < 0.01$ versus Andro.

zeta potential of AndroNLCs (-33.33 mV) compared to the Blank formulation (-25.11 mV) suggests enhanced stability due to stronger electrostatic repulsion, which reduces the likelihood of aggregation in nanofluids and colloidal systems[28,29] (Fig. 1B-C). This is crucial for maintaining the integrity and performance of the nanoparticles during storage and administration, including oral delivery routes[30,31].

Moreover, coupled with the high encapsulation efficiency achieved, this is a noteworthy accomplishment, enhancing both drug loading capacity and stability. The high encapsulation efficiency of Andro in NLCs (89.11%) demonstrates effective loading of the active compound into the NLCs. Although encapsulation efficiency for hydrophobic drugs can exceed 90%, this typically requires a higher material-to-drug ratio[32]. The efficiency in this study is commendable and indicates that Andro is effectively loaded into the NLCs while potentially using a more balanced material-to-drug ratio[26,32,33]. This level of efficiency is beneficial for maximizing the drug payload, improving therapeutic outcomes, and reducing required dosages.

Interestingly, AndroNLCs exhibit remarkable stability in both simulated gastric and intestinal conditions, maintaining structural integrity and uniform dispersion (Fig. 1D). In SGF, there was a slight increase in particle size from 131.40 ± 2.50 to 134.18 ± 2.17 nm, while the PdI remained stable (0.17 ± 0.02 to 0.18 ± 0.01), indicating resistance to acidic conditions and pepsin. Similarly, in SIF, there was a slight increase in particle size from 131.40 ± 2.50 to 141.10 ± 5.00 nm, and there were minimal changes in PdI (0.17 ± 0.02 to 0.20 ± 0.01), indicating stability against pancreatin and bile salts. The highly negative zeta potential of AndroNLCs prevents aggregation, ensuring effective delivery of therapeutic payloads in the gastrointestinal tract, rendering them suitable candidates for oral delivery systems targeting neuroinflammation-mediated disorders[34–36]. These findings demonstrate the suitability of AndroNLCs as a delivery system for Andro. The controlled particle size, enhanced stability through zeta potential, and efficient encapsulation highlight its potential for targeted and sustained drug release applications. This can particularly benefit bioavailability, prolong drug action, and minimize the side effects of conventional formulations.

This study assesses the safety and efficacy of AndroNLCs, emphasizing cytotoxicity results and the potential to mitigate inflammation before animal model testing. The findings suggest that AndroNLCs display a favorable safety profile, exhibiting reduced cytotoxicity in comparison to the Blank and Andro treatments (Fig. 2A). At concentrations where cell viability is reduced to 80% or less, AndroNLCs consistently showed better performance[23,37,38]. Specifically, cell viability was slightly higher for Andro compared to Blank and AndroNLCs at 31 ppm. In comparison, 250 ppm AndroNLCs demonstrated greater benefits in cell viability compared to both Blank and Andro. These findings suggest that AndroNLCs could reduce cytotoxicity, making AndroNLCs a potentially safer option for therapeutic applications in the in vivo studies. Consistent with the results, the observed changes in liver function indicate that AndroNLCs reduced hepatotoxicity caused by TNF-alpha-induced inflammation in mice (Figure F3J). Not only did Andro in NLCs demonstrate cytotoxic safety, but they also exhibited anti-inflammatory-like action by significantly lowering high levels of IL-6 and TNF-alpha in LPS-pretreated cells, with reductions observed at both 2.5 μg/mL and 5 μg/mL doses (as shown in Fig. 2B-C). These

results indicate that AndroNLCs may be more effective than natural Andro in reducing inflammation while maintaining cell viability in inflammatory conditions[37,38].

Despite these promising results, further studies are needed to assess the ability of AndroNLCs to cross the BBB, as effective BBB penetration is essential for treating neurological disorders. Solid lipid nanoparticles with Andro encapsulation may facilitate targeted delivery to the BBB. Time-dependent internalization studies of NLCs could reveal AndroNLCs' potential for BBB penetration, making them a valuable candidate for treating neuroinflammation and related conditions[35,39]. Additionally, Andro exhibits low oral bioavailability across species, limiting its systemic effects[40,41]. In mice, oral administration of 50 mg/kg (142.73 μmol/kg) resulted in poor bioavailability (9.27 ± 1.69%), with a peak plasma concentration of 0.73 ± 0.17 μmol/L at 0.42 ± 0.14 h, indicating rapid absorption but limited systemic exposure[41].To overcome these limitations, this study will further assess the pharmacokinetic properties of AndroNLCs, focusing on absorption, distribution, metabolism, and excretion in this novel delivery system.

Recent studies demonstrate a significant association between inflammation and sickness behavior in animal models, as reviewed by Rafiyan et al.[42] Inflammation in rodents, induced by methods such as cancer, endotoxin LPS, or ovalbumin-induced food allergy, results in symptoms like reduced weight gain, similar to those observed with TNF-alpha injection (Fig. 3C-D), indicating sickness[13]. Our study further reveals a significant connection between the pro-inflammatory cytokine TNF-alpha and behavioral abnormalities in animal studies. Mice with TNF-alpha-induced inflammation exhibited hyperactivity in the adrenal gland, spleen, thymus, and liver, as indicated by increased organ weights during the immune-inflammatory challenge (Fig. 3E-G). This was accompanied by elevated serum CORT levels, altered liver function profiles, increased pro-inflammatory cytokines (i.e., IL-6 and TNF-alpha), and heightened oxidative stress (i.e., MDA) in the hippocampus (Fig. 3H-M). Consequently, these results are reflected in increased locomotor activity and rearing in the OFT, along with generalized anxiety-like behavior in the ETM and depression-like behaviors in the TST and FST (Fig. 4). Consistently, previous studies show that increasing TNF-alpha levels peripherally, either through intraperitoneal injection or osmotic pumps, induces a robust inflammatory response marked by high levels of TNF-alpha, IL-6, and monocyte chemoattractant protein (MCP-1). These findings confirm that TNF-alpha leads to sickness behavior, characterized by reduced weight gain, altered emotional states (e.g., anxiety- and depression-like behavior), and presumably impaired memory consolidation[10,13,43].

From studies using LPS to induce inflammation support this connection, as systemic LPS exposure also leads to sickness behavior in mice[44], indicating a common inflammatory pathway affecting behavior. The role of TNF-alpha in behavior becomes more nuanced when considering TNF receptor deletion. Patel et al.[45] found that mice lacking TNF-R1 and TNF-R2 receptors showed increased non-aggressive exploration and anxiolytic-like behaviors, suggesting these receptors regulate anxiety-related behaviors. Sustained high levels of IL-6 and TNF-alpha in the hippocampus can activate the HPA axis, leading to increased CORT release[4,46]. The CORT, a stress hormone, contributes to sickness behavior symptoms, including reduced weight gain, and can cause imbalances in central norepinephrine and serotonin, leading to anxiety and depression-like behaviors[8,9,47]. Additionally, elevated CORT, inflammation, and oxidative stress contribute to hippocampal injury by decreasing pyramidal layer thickness, reducing cell survival, and increasing pyknotic cells, potentially leading to behavioral abnormalities[4,23,48].

In addition to validating animal models for inducing inflammation, exploring alternative therapeutic treatments with fewer side effects and effective anti-inflammatory properties is crucial. *Andrographis paniculata* (Burm. f) Nees-derived natural Andro has been widely used as a medicinal herb in various traditional systems, renowned for attenuating inflammation and oxidative stress[17,20,49]. Although body weight gain and feed consumption did not change during a 65-day administration of Andro in healthy rats[50], the present study demonstrated that both Andro and AndroNLCs could restore body weight reduction in mice with TNF-alpha-induced inflammation over a 14-day period (Fig. 3C-D). This suggests that these AndroNLC formulations may effectively mitigate inflammation-induced weight changes, which are indicative of sickness.

Despite a significant reduction in hippocampal TNF-alpha levels, the natural Andro formulation's limited pharmacological effects were due to poor solubility and absorption. This resulted in a less pronounced reduction in serum CORT levels and a marked increase in hippocampal IL-6 and MDA levels. However, AndroNLCs enhanced efficacy by reducing all stress-, inflammatory-, and oxidative stress-related markers. In general, the standard anti-inflammatory treatment with DEXA directly attenuates inflammation and can mitigate stress associated with sepsis or infection[51]. DEXA can also exhibit partial anti-stress effects, as shown by reduced serum CORT, MDA levels and decreased anxiety-like and panic-like behaviors in the OFT and ETM. However, despite these effects, which are associated with elevated hippocampal IL-6 and MDA levels, AndroNLCs demonstrated superior effectiveness. As expected, VLX has been shown to modulate the balance of central norepinephrine and serotonin, promoting neuroprotection and attenuating CORT levels and anxiety-related behavior similarly to DEXA. However, it does not mitigate inflammatory and oxidative stress markers as effectively in this animal study[52,53]. Additionally, AndroNLCs outperformed the monoamine-modulating antidepressant VLX (Fig. 3H-J). Consequently, AndroNLCs exhibited notable anxiolytic- and antidepressant-like actions, similar to VLX and DEXA treatments, as indicated by shortened escape times in the ETM and reduced immobility in the TST (Fig. 4F-H).

Besides behavioral and biochemical improvements, Andro could alleviate BBB disruption and neuronal cell damage[18,19,21,54]. Particularly, Andro in NLCs may further enhance hippocampal neuroprotection against systemic inflammation by attenuating behavioral abnormalities and cognitive deficits, reducing acetylcholinesterase activity, and mitigating oxidative stress, as observed in diabetic rats. Additionally, Andro can enhance hippocampal BDNF signaling in rats with cerebral hypoperfusion[55]. Furthermore, Andro in NLCs could increase cell proliferation in the dentate gyrus, as indicated by markers such as BrdU, doublecortin, and Ki67 cells in the hippocampal *APPswe/PSEN1ΔE9* mice[19,55–57]. These mechanisms may contribute to increasing

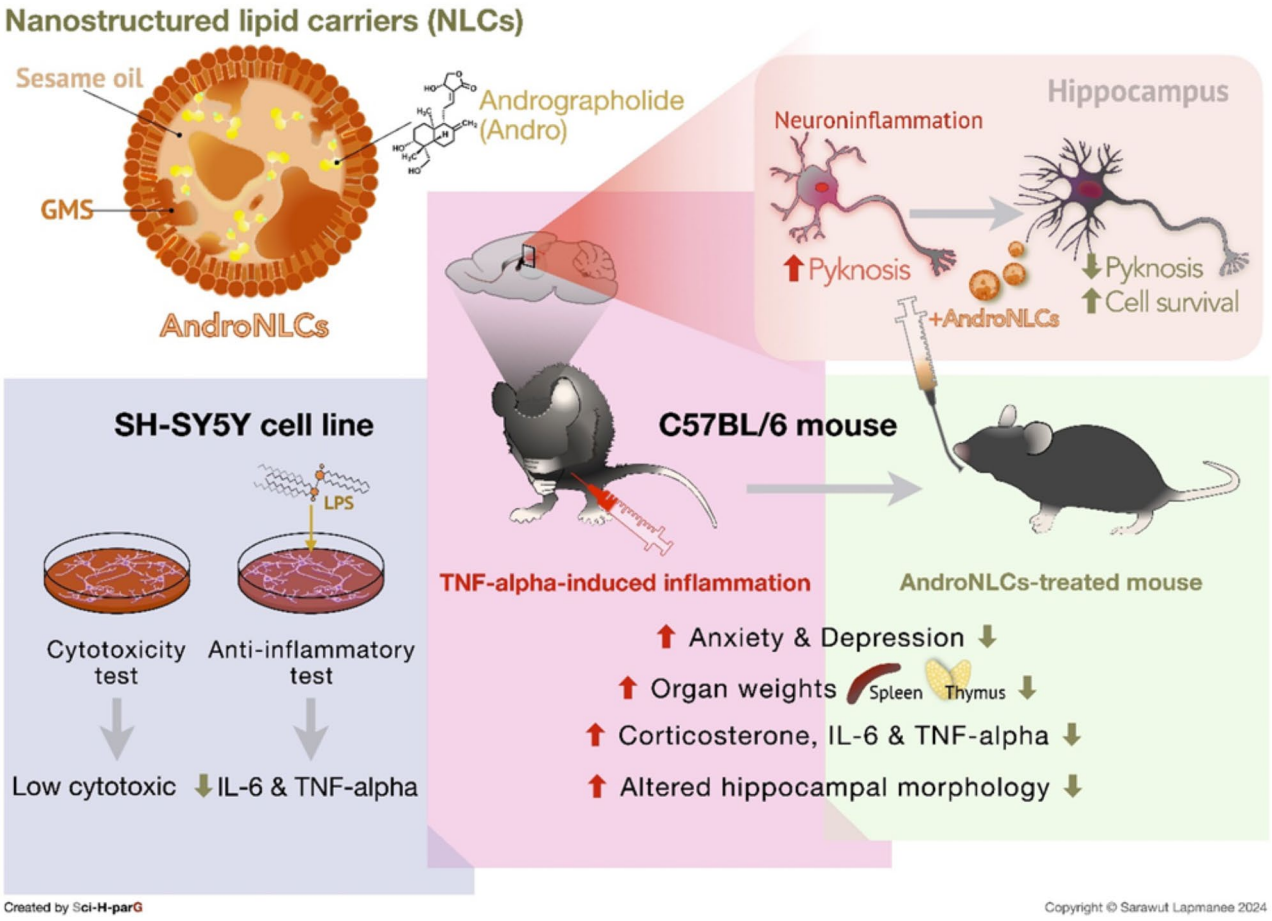

Fig. 6. The summary of the study shows the composition, which includes andrographolide (Andro), sesame oil, and glycerol monostearate (GMS). This representation demonstrates the effectiveness of Andrographolide-loaded nanostructured lipid carriers (AndroNLCs), showing low cytotoxicity and significant anti-inflammatory effects in lipopolysaccharide (LPS)-pretreated SH-SY5Y neuroblastoma cell cultures, with reduced levels of interleukin-6 (IL-6) and tumor necrosis factor-alpha (TNF-alpha). Additionally, AndroNLCs effectively alleviated anxiety, depression, and compensatory responses to TNF-alpha challenge in male C57BL/6 mice. This was demonstrated by decreased targeted organ weights, reduced corticosterone, lower hippocampal IL-6, TNF-alpha, oxidative stress levels, and improved hippocampal morphology and pyknosis with increased cell survival, suggesting potential for mitigating neuroinflammation-induced behavioral abnormalities.

survival cells and attenuating hippocampal neural damage, including a reduction in hippocampal layer thickness and the presence of pyknotic cells in mice with TNF-alpha-induced inflammation (Fig. 5; Table 1).

As summarized in Fig. 6, our findings revealed the potential benefits of innovative AndroNLCs, a formulation characterized by improved encapsulation, homogeneity, stability, enhanced oral efficacy, low toxicity, and mitigation of inflammation in an in vitro study. The present study also demonstrated the therapeutic efficacy of AndroNLCs in reducing inflammation induced by TNF-alpha and alleviating sickness and stress-related behaviors associated with anxiety and depression in an in vivo study. This AndroNLC formulation was shown to mitigate hippocampal neuronal deterioration. However, further studies are necessary to assess the long-term effects of AndroNLCs, particularly concerning their toxicity and efficacy in models of systemic inflammation. Additionally, ongoing research aims to elucidate the specific mechanisms of AndroNLCs, particularly the interaction with the TNF-alpha signaling pathway, in modulating antipsychotic effects and memory impairment under inflammatory conditions. Molecular techniques and comprehensive histological evaluations, including the assessment of gene and protein expression regulating brain plasticity, as well as Nissl staining and TUNEL assays, would be employed in these studies. Taken together, by enhancing the delivery and therapeutic efficacy of Andro, AndroNLCs could serve as a novel alternative to current treatments for patients suffering from neuroinflammation caused by systemic inflammation.

Materials and methods

Preparation and characterization of AndroNLCs

AndroNLCs were prepared using high-pressure homogenization. Briefly, glycerol monostearate, black sesame oil (Catalog number: 1612415, Product Code: 41116107), sorbitan oleate (Catalog number: S6760,

Product Code: 12161900), and Andro (98% Andrographolide, Catalog No. 365645, Lot# MKCH1668, Product Code: 1002817134) from Sigma-Aldrich, St. Louis, MO, USA were heated together at 60 to 80 °C in a 10:5:2:1 weight ratio to form the lipid phase. The co-surfactant from Sigma-Aldrich, St. Louis, MO, USA, Polysorbate 80 (Catalog number: 1.37171, Product Code: 12352207), and iodopropynyl butylcarbamate (Catalog number: PHR1354, Product Code: 41116107), were heated in deionized water (DI), forming the aqueous phase. This aqueous phase was then added to the lipid phase, and the mixture was sonicated using a probe at 35% amplitude for 30 min.

The particle size, polydispersity index (PdI) and zeta potential of NLCs were determined using a dynamic light scattering (DLS) Nanosizer (Malvern Panalytical Ltd., Malvern, UK). The particle suspension was diluted 1,000 times in DI water before the analysis. All measurements were performed in triplicates. Additionally, the DLS technique confirmed the stability of AndroNLCs, following storage at 25 °C for 3 months[23]. The particle morphology of AndroNLCs was characterized using a transmission electron microscope (TEM, JEM-2100 plus, JEOL, Osaka, Japan) after vacuum-drying. The TEM samples were diluted in DI water and dropped on a copper grid, and the samples were observed at a magnification of 40,000× and at 200 kV.

The encapsulation efficiency (EE) of AndroNLCs was determined using an Amicon membrane filter, followed by centrifugation. Unloaded Andro in the aqueous phase was filtered, and AndroNLCs concentration was evaluated and calculated based on HPLC-UV analysis. The encapsulation efficiency was calculated using the following equation:

$$\%EE = \frac{C_i - C_F}{C_i} \times 100$$

Where C_i is the initial concentration of Andro added to NLCs. C_f is the concentration of unloaded Andro.

Measurement of the stability of AndroNLCs in simulated gastric and intestinal conditions

The stability in simulated gastric and intestinal conditions was performed following in vitro digestion protocol as described by Minekus et al.[58] The NLCs were soaked in simulated gastric fluid (SGF, pH 3) and simulated intestinal fluid (SIF, pH 7) at 37 °C in a shaking incubator for 4 h. Particle size, PdI and zeta potential of NLCs were monitored the stability in simulated fluids. The measurements were repeated in triplicate, and the average values were calculated. The stability of the encapsulated AndroNLCs in simulated gastric or intestinal conditions was performed by mixing 0.5 mL of samples with 0.5 mL of SGF or SIF stock solution to make a final AndroNLC concentration of 0.5 mg/mL. The mixtures were fully incubated with shaking incubator at 500 rpm, 37 °C for 2 h. Particle size, PdI and zeta potential of AndroNLCs were measured as mentioned above.

Measurement of in vitro cytotoxicity and inflammatory responses.

The human SH-SY5Y neuroblastoma cell line from American Type Culture Collection company, VA, USA (ATTC: CRL-2266) was maintained in Eagle's Minimum Essential Medium supplemented with 10% fetal bovine serum (Gibco™, Catalog number: A5670701, Lot number: U3090991RP, Life Technologies Corporation, NY, USA), 100 units/mL penicillin and 100 µg/mL streptomycin (Pen&Strep, Gibco™, Catalog number: 15070063, Lot number: 240298, Life Technologies Corporation, NY, USA). Cells were cultured at 37 °C in a 5% CO_2 incubator. Cytotoxicity of neuron cells was evaluated by the MTT (3-(4,5-dimethylthiazol-2-yl)-2,5-diphenyltetrazolium bromide) tetrazolium reduction assay (Catalog number: M6494, Lot number: 78952442, Invitrogen™,Life Technologies, OR, USA), which measured mitochondrial succinate dehydrogenase. Cells were seeded at a density of 1×10^4 cells/well in 96-well plates and allowed to grow until 70–80% confluent, followed by treatment with Blank, isolated Andro and AndroNLCs. Cytotoxicity was examined 24 h post incubation by adding 100 µL MTT solution (1 mg/mL in PBS) to each well and incubating for 4 hours at 37 °C. MTT solution was removed, and the formazan crystals were dissolved by adding 100 µL DMSO to each well. Finally, the absorbance was measured at 570 nm using SpectraMax M2 microplate readers (Molecular Devices LLC, San Jose, CA, USA)[23].

After differentiating SH-SY5Y cells, pre-treatment was conducted with LPS (*E. coli* O55:B5, Catalog number: L2637, Product code: 12352201, Sigma-Aldrich, St. Louis, MO, USA) at a 1 µg/mL concentration. The cells were cultured for 24 h, with untreated cells serving as controls. Following treatment with either 2.5–5 µg/mL of Andro or AndroNLCs, the culture media from both treated and control cells were collected and stored at − 80 °C until measurement. The concentrations of IL-6 and TNF-alpha secreted into the culture media of SH-SY5Y monocultures were measured using human IL-6 (catalog number EH2IL6) and TNF-alpha (catalog number 88-7346-88) ELISA Kits (Invitrogen, Thermo Fisher Scientific Inc., MA, USA), following the manufacturer's instructions[59].

Animal and treatments

Fifty-four adult male C57BL/6 mice (8 weeks old) were purchased from Nomura Siam International Co., Ltd. (Bangkok, Thailand). The mice were randomly housed in groups (9 mice/group) in a controlled standard animal laboratory room maintained at 23 ± 2 °C and 54 ± 3% humidity, with a 12-hour day/night cycle. The mice were fed a standard chow diet from Charoen Pokphand Foods Public Co., Ltd. (Bangkok, Thailand) for at least 7 days before the start of the experiments. The experimental procedures were approved by the Institutional Animal Care and Use Committee of Thammasat University, Pathum Thani, Thailand (project number 21-2021, renewed in 2024). The Laboratory Animal Center at Thammasat University is internationally accredited by AAALAC. All experiments and methods performed in this study complied with relevant regulations and adhered to the

ARRIVE (Animal Research: Reporting of in vivo experiments) guidelines. The mice were randomly assigned to six groups as follows:

1. Control group: mice received a sterile phosphate-buffered saline (PBS) intraperitoneal injection (i.p., 1 mL/kg) for inflammation induction coupled with a daily oral dose of 3 mL/kg lipid solution (vehicle) for 14 days.
2. Vehicle group: mice received 63 µg/kg TNF-alpha (i.p.) every three days for a total of 12 days (5 doses) coupled with a daily oral dose of 3 mL/kg lipid solution for 14 days.
3. Andrographolide group (Andro): inflamed mice received a daily oral dose of 10 mg/kg Andro in lipid solution for 14 days.
4. Andrographolide-loaded lipid nanoparticles group (AndroNLCs): inflamed mice received a daily oral dose of 10 mg/kg AndroNLCs for 14 days.
5. Dexamethasone group (DEXA): inflamed mice received a daily oral dose of 1 mg/kg DEXA, a positive control for systemic inflammation for 14 days.
6. Venlafaxine group (VLX): inflamed mice received a daily oral dose of 10 mg/kg VLX as a positive control for stress-reducing effects (anti-stress monoamine modulator) for 14 days.

After completing the treatment period, all mice were assessed for stress-related behaviors, including locomotor activity and anxiety- and depression-like behaviors, using the open-field test (OFT), the elevated T-maze (ETM), the tail suspension test (TST), and the forced swimming test (FST). Following the 24-hour behavioral tests, the mice were euthanized using isoflurane inhalation. Blood and target organs (brain, thymus, and spleen) were then collected to investigate immune defense mechanisms during an inflammatory challenge. Specifically, five fresh hippocampal tissue samples were subjected to biochemical analysis, while four samples underwent the embedding process in paraffin for histological study[4].

Administration of anti-inflammatory medications in mice with TNF-alpha-induced neuroinflammation

Based on Biesmans et al.[13], a dose of 63 µg/kg TNF-alpha (i.p.) induced sickness, systemic inflammation, and behavioral abnormalities. This dose significantly affected brain and serum levels of IL-6, TNF-alpha, and MCP-1 and influenced IFN-γ levels in the brain, indicating its effectiveness in inducing an inflammatory response. Recombinant mouse TNF-alpha (aa 80–235) protein (catalog number 410-MT-010, R&D Systems, Inc., Minnesota, USA) dissolved in sterile PBS and administered every 3 days for a total of 5 doses. In parallel, the mice were orally administered 10 mg/kg Andro (Sigma-Aldrich, Missouri, USA) and 10 mg/kg AndroNLCs (in a 1 mg/mL formulation), along with the standard anti-inflammatory DEXA, 1 mg/kg from Charoen Pharmacy Lab Company, Bangkok, Thailand[51], and the antidepressant VLX, 10 mg/kg from Pfizer Ireland Pharmaceuticals, Co. Kildare, Ireland, which is a serotonin and norepinephrine reuptake inhibitor[4]. Andro or AndroNLCs were administered orally based on anxiolytic action by reducing stress-induced hyperthermia and sleep disturbances, comparable to diazepam[60]. AndroNLCs, with an 89% Andro load, were administered at 0.28 mL of the 1 mg/mL formulation to a 25 g mouse, delivering 0.25 mg of andrographolide (10 mg/kg). These treatments were given daily between 9:00 AM and 12:00 PM for 14 days.

Measurement of stress-related behaviors

Locomotor activity and anxiety-like behaviors

Open-field test (OFT) The open field apparatus was used to study motor activity and anxiety levels in response to an unfamiliar environment on day 15. The apparatus was a square enclosure made of black acrylic plastic, measuring 100 × 100 × 40 cm. The floor was divided by white lines arranged in a 20 × 20 pattern, with each square being 5 × 5 cm. The inner zone was defined as a 90 × 90 cm square located 5 cm from each wall, with the remaining area designated as the outer zone. The open field was illuminated by a neon tube lamp, providing 200 lx in the center of the field. To begin the test, each mouse was gently placed in the central area and allowed to explore for 5 min. All behavioral profiles were recorded using an infrared digital video camera positioned above the open field. After each trial, the open field apparatus was cleaned with a paper towel soaked in 20% alcohol. The total number of line crosses and rearing was used to indicate locomotor activity and exploration. Additionally, increased time spent in the outer arena was used as an indicator of higher anxiety levels[52,53].

Elevated T-maze (ETM) To study different types of anxiety (i.e., conditioned or learned fear associated with generalized anxiety and unconditioned fear or panic-like behaviors) in mice, the ETM was used following the OFT with a 1-hour resting period on day 15. The ETM was constructed from black acrylic plastic and consisted of three parts: two enclosed arms with opaque walls and two open arms positioned perpendicularly to the enclosed arms. The apparatus was elevated 50 cm above the floor. To prevent falls, the open arms were surrounded by a 1 cm high Plexiglas rim. Between trials with different mice, the apparatus was cleaned with 20% alcohol. Each mouse was tested only once and gently placed in the ETM. The procedure involved measuring three trials of inhibitory avoidance acquisition: baseline latency, avoidance latency I, and avoidance latency II, with 30-second resting intervals between trials. Additionally, one-way escape latency was assessed following the inhibitory avoidance test. In the ETM, all tests were recorded with a maximum 5 min per trial. Generalized anxiety-like behavior was defined as increased latencies to leave the enclosed arm across these trials, while panic-like behavior was characterized by decreased one-way escape latency from an open arm[53].

Depression-like behaviors

Following ETM test, the tail suspension test (TST) was conducted on day 16, to assess despair-related behaviors under inescapable stress. The tail was suspended using adhesive tape placed 1 cm from the tip. A stainless-

steel stand, 45 cm high, ensured consistent tail suspension, with each mouse hanging 40 cm above the ground. Immobility, defined as the absence of any movement except for breathing, was recorded for 6 min using a digital video camera. Increased immobility time is considered an indicator of depression-like behavior in mice[61].

To further confirm depressive-like behavior in mice induced by environmental hopelessness, a 6-minute forced swimming test (FST) was conducted after the 1-hour TST. Mice were assessed individually in bright plastic cylinders (45 cm in height and 20 cm in diameter) filled with 30 cm of 25 °C tap water. Immobility behavior (floating with only minimal movements necessary to keep the head above water) in FST was recorded using a digital video camera. An increase in immobility duration indicated higher levels of depression-like behavior[62].

Euthanasia

The mice were euthanized using an overdose of isoflurane anesthesia (Attane™, Missouri, USA), administered via inhalation. Anesthesia induction involved inhaling 5% vaporized isoflurane. Before blood and specimen collection, the mice showed no movements or reactions to pain stimuli at the foot and tail.

Measurement of body and organ weights

The body weight of the mice was recorded daily throughout the 16-day experiment. The percentage change in daily body weight gain was then determined by calculating the difference between the weight at the end of the acclimation period and the weight at the study endpoint. Following euthanasia, the adrenal glands, spleen and thymus of each mouse were excised and weighed. These organs serve as indicators of systemic immunotoxicity and stress responses. Organ weights relative to the final body weight allow for accurate interpretations of organ size and function in relation to overall body weight[4].

Measurement of stress, toxicity, inflammatory, and oxidative stress markers

Blood was carefully conducted via cardiac puncture between 9:00 AM and 12:00 PM, and serum was prepared. While the dorsal part of the hippocampi was microdissected and lysed. The supernatant was collected for pro-inflammatory cytokine analysis. Serum corticosterone (CORT) levels, along with hippocampal TNF-alpha and IL-6 levels, were assessed using commercial immunoassay kits, corticosterone parameter assay kits (catalog number KGE009, R&D Systems, Inc., Minnesota, USA), mouse TNF-alpha ELISA 96T/kit (catalog number ELM-TNFa-CL-1, RayBiotech Life, Inc., Georgia, USA) and mouse IL-6 ELISA, 96TKit (catalog number ELM-IL6-1, RayBiotech Life, Inc., Georgia, USA) following the respective manufacturer's instructions. In addition, serum was prepared for blood chemistry analysis, i.e., alanine aminotransferase (ALT) and aspartate aminotransferase (AST), conducted using a chemistry analyzer (BS-620 M, China). Malondialdehyde (MDA) levels were determined by constructing a standard curve using 1,1,3,3-tetraethoxypropane in the 0.3 to 1 µmol/L. MDA concentrations in the hippocampal supernatant were normalized to the protein concentration, which was determined using the Bradford dye-binding method.

Measurement of hippocampal neuronal morphology

Following euthanasia, blood was collected from the mice via cardiac puncture. The mice brains were washed with cold 0.1 M PBS at pH 7.4, and the brain hemispheres were then immersed overnight in 4% paraformaldehyde in 0.1 M PBS. Brains from each experimental group ($n = 4$) were subsequently processed for paraffin embedding. Brain sections with a thickness of 5 µm were manually cut using a rotary microtome (Leica Biosystems, Nussloch, Germany). Hippocampal sections were stained with standard hematoxylin and eosin (H&E, MilliporeSigma, Massachusetts, USA) to evaluate alterations in neuronal morphology in the cornu ammonis (CA) 1 to 4 regions and the dentate gyrus (DG). The pyramidal cell layer (PCL) and granular cell layer (GCL) thickness, the number of surviving cells, and the presence of neuronal injury or damage, as represented by pyknotic cells, were photographed with a light microscope and assessed using ImageJ software[4,23].

Statistical analysis

Data are reported as mean ± standard error of the mean (SEM). Unpaired Student's t-tests were used to compare two data sets, while one-way analysis of variance (ANOVA) with Dunnett's multiple comparison test was used to compare group differences. Normality tests were conducted to assess whether the data followed a Gaussian distribution. Statistical significance was set at $P < 0.05$. All statistical analyses and graphical representations were performed using GraphPad Prism 10 (GraphPad Software Inc., San Diego, CA, USA).

Data availability

Datasets and analyses from this study are not publicly available due to a pending patent filing but can be provided upon reasonable request from the corresponding author.

Received: 19 August 2024; Accepted: 31 March 2025
Published online: 08 April 2025

References

1. Chen, L. et al. Inflammatory responses and inflammation-associated diseases in organs. *Oncotarget* **9**, 7204–7218. https://doi.org/10.18632/oncotarget.23208 (2017).
2. Oronsky, B., Caroen, S. & Reid, T. What exactly is inflammation (and what is it not?). *Int. J. Mol. Sci.* **23**, 14905. https://doi.org/10.3390/ijms232314905 (2022).
3. Ye, Z. et al. Role of inflammation in depression and anxiety: Tests for disorder specificity, linearity and potential causality of association in the UK biobank. *EClinicalMedicine* **38**, 100992. https://doi.org/10.1016/j.eclinm.2021.100992 (2021).

4. Lapmanee, S. et al. Stress-induced changes in cognitive function and intestinal barrier integrity can be ameliorated by Venlafaxine and synbiotic supplementations. *PeerJ* **12**, e17033. https://doi.org/10.7717/peerj.17033 (2024).
5. Maydych, V. The interplay between stress, inflammation, and emotional attention: Relevance for depression. *Front. Neurosci.* **13**, 384. https://doi.org/10.3389/fnins.2019.00384 (2019).
6. Ravi, M., Miller, A. H. & Michopoulos, V. The immunology of stress and the impact of inflammation on the brain and behavior. *BJPsych. Adv.* **27**, 158–165. https://doi.org/10.1192/bja.2020.82 (2021).
7. Rhie, S. J., Jung, E. Y. & Shim, I. The role of neuroinflammation on pathogenesis of affective disorders. *J. Exerc. Rehabil.* **16**, 2–9. https://doi.org/10.12965/jer.2040016.008 (2020).
8. Jeon, S. W. & Kim, Y. K. Neuroinflammation and cytokine abnormality in major depression: Cause or consequence in that illness? *World J. Psychiatry* **6**, 283–293. https://doi.org/10.5498/wjp.v6.i3.283 (2016).
9. Tseilikman, V. et al. Role of glucocorticoid- and monoamine-metabolizing enzymes in stress-related psychopathological processes. *Stress* **23**, 1–12. https://doi.org/10.1080/10253890.2019.1641080 (2020).
10. Klaus, F. et al. Differential effects of peripheral and brain tumor necrosis factor on inflammation, sickness, emotional behavior and memory in mice. *Brain Behav. Immun.* **58**, 310–326. https://doi.org/10.1016/j.bbi.2016.08.001 (2016).
11. He, J. et al. Oxidative stress and neuroinflammation potentiate each other to promote progression of dopamine neurodegeneration. *Oxid. Med. Cell. Longev.* **2020**, 6137521. https://doi.org/10.1155/2020/6137521 (2020).
12. Tartt, A. N. et al. Dysregulation of adult hippocampal neuroplasticity in major depression: Pathogenesis and therapeutic implications. *Mol. Psychiatry* **27**, 2689–2699. https://doi.org/10.1038/s41380-022-01520-y (2022).
13. Biesmans, S. et al. Peripheral administration of tumor necrosis factor-alpha induces neuroinflammation and sickness but not depressive-like behavior in mice. *BioMed. Res. Int.* 716920 (2015). https://doi.org/10.1155/2015/716920 (2015).
14. Kushner, P. et al. The use of non-steroidal anti-inflammatory drugs (NSAIDs) in COVID-19. *NPJ Prim. Care Respir Med.* **32**, 35. https://doi.org/10.1038/s41533-022-00300-z (2022).
15. Kalra, S. et al. Pathogenesis and management of traumatic brain injury (TBI): Role of neuroinflammation and anti-inflammatory drugs. *Inflammopharmacology* **30**, 1153–1166. https://doi.org/10.1007/s10787-022-01017-8 (2022).
16. Sohail, R. et al. Effects of non-steroidal anti-inflammatory drugs (NSAIDs) and gastroprotective NSAIDs on the Gastrointestinal tract: A narrative review. *Cureus* **15**, e37080. https://doi.org/10.7759/cureus.37080 (2023).
17. Li, X. et al. Andrographolide, a natural anti-inflammatory agent: An update. *Front. Pharmacol.* **13**, 920435. https://doi.org/10.3389/fphar.2022.920435 (2022).
18. Bosco, F. et al. The effects of *Andrographis paniculata* (Burm.F.) wall. Ex Nees and Andrographolide on neuroinflammation in the treatment of neurodegenerative diseases. *Nutrients* **15**, 3428. https://doi.org/10.3390/nu15153428 (2023).
19. Arredondo, S. et al. Andrographolide promotes hippocampal neurogenesis and Spatial memory in the APPswe/PS1ΔE9 mouse model of Alzheimer's disease. *Sci. Rep.* **11**, 22904. https://doi.org/10.1038/s41598-021-01977-x (2021).
20. Gong, P. et al. Andrographolide attenuates blood–brain barrier disruption, neuronal apoptosis, and oxidative stress through activation of Nrf2/HO-1 signaling pathway in subarachnoid hemorrhage. *Neurotox. Res.* **40**, 508–519. https://doi.org/10.1007/s12640-022-00486-7 (2022).
21. Yan, Y., Fang, L. H. & Du, G. H. Andrographolide. In *Natural Small Molecule Drugs from Plants*, Vol 1, 357–362. (Springer, 2018). https://doi.org/10.1007/978-981-10-8022-7_60
22. Hossain, K. R., Alghalayini, A. & Valenzuela, S. M. Current challenges and opportunities for improved Cannabidiol solubility. *Int. J. Mol. Sci.* **24**, 14514. https://doi.org/10.3390/ijms241914514 (2023).
23. Lapmanee, S. et al. Assessing the safety and therapeutic efficacy of Cannabidiol lipid nanoparticles in alleviating metabolic and memory impairments and hippocampal histopathological changes in diabetic Parkinson's rats. *Pharmaceutics* **16**, 514. https://doi.org/10.3390/pharmaceutics16040514 (2024).
24. Songvut, P. et al. Enhancing oral bioavailability of Andrographolide using solubilizing agents and bioenhancer: Comparative pharmacokinetics of *Andrographis paniculata* formulations in beagle dogs. *Pharm. Biol.* **62**, 183–194. https://doi.org/10.1080/13880209.2024.2311201 (2024).
25. Mehta, M. et al. Lipid-based nanoparticles for drug/gene delivery: An overview of the production techniques and difficulties encountered in their industrial development. *ACS Mater. Au* **3**, 600–619. https://doi.org/10.1021/acsmaterialsau.3c00032 (2023).
26. Gumustas, M. et al. Effect of polymer-based nanoparticles on the assay of antimicrobial drug delivery systems. In *Multifunctional Systems for Combined Delivery, Biosensing and Diagnostics* 1, 67–108. (Elsevier, 2017).
27. Meng, X. et al. Pluronic F127 and D-α-tocopheryl polyethylene glycol succinate (TPGS) mixed micelles for targeting drug delivery across the blood brain barrier. *Sci. Rep.* **7**, 2964. https://doi.org/10.1038/s41598-017-03123-y (2017).
28. Danaei, M. et al. Impact of particle size and polydispersity index on the clinical applications of lipidic nanocarrier systems. *Pharmaceutics* **10**, 57 (2018). https://doi.org/10.3390/pharmaceutics10020057
29. Pochapski, D. J. et al. Zeta potential and colloidal stability predictions for inorganic nanoparticle dispersions: Effects of experimental conditions and electrokinetic models on the interpretation of results. *Langmuir* **37**, 13379–13389. https://doi.org/10.1021/acs.langmuir.1c02056 (2021).
30. Nguyen, V. H. et al. Nanostructured lipid carriers and their potential applications for versatile drug delivery via oral administration. *OpenNano* **8**, 100064. https://doi.org/10.1016/j.onano.2022.100064 (2022).
31. Mahor, A. et al. Nanostructured lipid carriers for improved delivery of therapeutics via the oral route. *J. Nanotechnol.* 1–35 (2023). (2023).
32. Li, X., Zhao, Y. & Zhao, C. Applications of capillary action in drug delivery. *iScience* **24**, 102810. https://doi.org/10.1016/j.isci.2021.102810 (2021).
33. Ezike, T. C. et al. Advances in drug delivery systems, challenges and future directions. *Heliyon* **9**, e17488. https://doi.org/10.1016/j.heliyon.2023.e17488 (2023).
34. Zhou, Z. et al. Statistical investigation of simulated fed intestinal media composition on the equilibrium solubility of oral drugs. *Eur. J. Pharm. Sci.* **99**, 95–104. https://doi.org/10.1016/j.ejps.2016.12.008 (2017).
35. Su, L. et al. Solid lipid nanoparticles enhance the resistance of oat-derived peptides that inhibit dipeptidyl peptidase IV in simulated gastrointestinal fluids. *J. Funct. Foods.* **65**, 103773 (2020).
36. Vanti, G. et al. Nanostructured lipid carriers can enhance oral absorption of Khellin, a natural pleiotropic molecule. *Molecules* **26**, 7657. https://doi.org/10.3390/molecules26247657 (2021).
37. Iwasawa, A., Ayaki, M. & Niwano, Y. Cell viability score (CVS) as a good indicator of critical concentration of Benzalkonium chloride for toxicity in cultured ocular surface cell lines. *Regul. Toxicol. Pharmacol.* **66**, 177–183. https://doi.org/10.1016/j.yrtph.2013.03.014 (2013).
38. Kamiloglu, S., Sari, G., Ozdal, T. & Capanoglu, E. Guidelines for cell viability assays. *Food Front.* **1**, 332–349 (2020).
39. Niazi, S. K. Non-invasive drug delivery across the blood-brain barrier: A prospective analysis. *Pharmaceutics* **15**, 2599. https://doi.org/10.3390/pharmaceutics15112599 (2023).
40. Chen, H. W. et al. Bioavailability of andrographolide and protection against carbon tetrachloride-induced oxidative damage in rats. *Toxicol. Appl. Pharmacol.* **280**, 1–9. (2014). https://doi.org/10.1016/j.taap.2014.07.024 (2014).
41. Banerjee, M. et al. Cytotoxicity and cell cycle arrest induced by andrographolide lead to programmed cell death of MDA-MB-231 breast cancer cell line. *J Biomed Sci.* 23 (2016). https://doi.org/10.1186/s12929-016-0257-0 (2016).
42. Rafiyan, M., Sadeghmousavi, S., Akbarzadeh, M. & Rezaei, N. Experimental animal models of chronic inflammation. *Curr. Res. Immunol.* **4**, 100063. https://doi.org/10.1016/j.crimmu.2023.100063 (2023).

43. Habbas, S. et al. Neuroinflammatory TNFα impairs memory via astrocyte signaling. *Cell* **163**, 1730–1741. https://doi.org/10.1016/j.cell.2015.11.023 (2015).
44. Kelly, K. A. et al. Prior exposure to corticosterone markedly enhances and prolongs the neuroinflammatory response to systemic challenge with LPS. *PloS One* **13**, e0190546. https://doi.org/10.1371/journal.pone.0190546 (2018).
45. Patel, A., Siegel, A. & Zalcman, S. S. Lack of aggression and anxiolytic-like behavior in TNF receptor (TNF-R1 and TNF-R2) deficient mice. *Brain Behav. Immun.* **24**, 1276–1280. https://doi.org/10.1016/j.bbi.2010.05.005 (2010).
46. Johnson, J. D., Barnard, D. F., Kulp, A. C. & Mehta, D. M. Neuroendocrine regulation of brain cytokines after psychological stress. *J. Endocr. Soc.* **3**, 1302–1320. https://doi.org/10.1210/js.2019-00053 (2019).
47. Lam, V. Y. Y. et al. Role of corticosterone in anxiety- and depressive-like behavior and HPA regulation following prenatal alcohol exposure. *Prog. Neuropsychopharmacol. Biol. Psychiatry*. **90**, 1–15 (2019).
48. Chesnokova, V., Pechnick, R. N. & Wawrowsky, K. Chronic peripheral inflammation, hippocampal neurogenesis, and behavior. *Brain Behav. Immun.* **58**, 1–8. https://doi.org/10.1016/j.bbi.2016.01.017 (2016).
49. Zhang, J. J. et al. Andrographolide exerts significant antidepressant-like effects involving the hippocampal BDNF system in mice. *Int. J. Neuropsychopharmacol.* **22**, 585–600. https://doi.org/10.1093/ijnp/pyz032 (2019).
50. Dey, Y. N., Kumari, S., Ota, S. & Srikanth, N. Phytopharmacological review of *Andrographis paniculata* (Burm.f) wall. Ex Nees. *Int. J. Nutr. Pharmacol. Neurol. Dis.* **3** (2013).
51. Katagiri, H. et al. Modulation of serotonin2A receptor function in rats after repeated treatment with dexamethasone and L-type calcium channel antagonist nimodipine. *Prog Neuropsychopharmacol. Biol. Psychiatry*. **25**, 1269–1281. https://doi.org/10.1016/s0278-5846(01)00179-8 (2001).
52. Lapmanee, S., Charoenphandhu, J., Teerapornpuntakit, J., Krishnamra, N. & Charoenphandhu, N. Agomelatine, venlafaxine, and running exercise effectively prevent anxiety- and depression-like behaviors and memory impairment in restraint stressed rats. *PloS One* **12**, e0187671. https://doi.org/10.1371/journal.pone.0187671 (2017).
53. Lapmanee, S. et al. Venlafaxine and synbiotic attenuated learned fear-like behavior and recognition memory impairment in immobilized-stressed rats. *Physiol. Pharmacol.* **27**, (2023).
54. Das, S., Mishra, K. P., Ganju, L. & Singh, S. B. Andrographolide—A promising therapeutic agent, negatively regulates glial cell derived neurodegeneration of prefrontal cortex, hippocampus and working memory impairment. *Neuroimmunol* **313**, 161–175. https://doi.org/10.1016/j.jneuroim.2017.11.003 (2017).
55. Wang, D. P. et al. Andrographolide enhances hippocampal BDNF signaling and suppresses neuronal apoptosis, astroglial activation, neuroinflammation, and Spatial memory deficits in a rat model of chronic cerebral hypoperfusion. *Naunyn Schmiedebergs Arch. Pharmacol.* **392**, 1277–1284. https://doi.org/10.1007/s00210-019-01672-9 (2019).
56. Varela-Nallar, L., Arredondo, S. B., Tapia-Rojas, C., Hancke, J. & Inestrosa, N. C. Andrographolide stimulates neurogenesis in the adult hippocampus. *Neural Plast*. 935403 (2015). https://doi.org/10.1155/2015/935403 (2015).
57. Thakur, A. K., Rai, G., Chatterjee, S. S. & Kumar, V. Beneficial effects of an andrographis paniculata extract and Andrographolide on cognitive functions in streptozotocin-induced diabetic rats. *Pharm. Biol.* **54**, 1528–1538. https://doi.org/10.3109/13880209.2015.1107107 (2016).
58. Minekus, M. et al. A standardised static in vitro digestion method suitable for food—An international consensus. *Food Funct.* **5**, 1113–1124 (2014).
59. Pandur, E. et al. Effect of inflammatory mediators lipopolysaccharide and Lipoteichoic acid on iron metabolism of differentiated SH-SY5Y cells alters in the presence of BV-2 microglia. *Int. J. Mol. Sci.* **20**, 17. https://doi.org/10.3390/ijms20010017 (2018).
60. Thakur, A. K., Chatterjee, S. S. & Kumar, V. Adaptogenic potential of andrographolide: An active principle of the King of bitters (*Andrographis paniculata*). *J. Tradit Complement. Med.* **5**, 42–50. https://doi.org/10.1016/j.jtcme.2014.10.002 (2014).
61. Ueno, H. et al. Effect of simultaneous testing of two mice in the tail suspension test and forced swim test. *Sci. Rep.* **12**, 9224. https://doi.org/10.1038/s41598-022-12986-9 (2022).
62. Songphaeng, T. et al. Atomoxetine and Escitalopram migrate the derangement of the temporomandibular joint morphologic and histologic changes in rats exposed to stress-induced depression. *J. Oral Sci.* **65**, 219–225. https://doi.org/10.2334/josnusd.23-0077 (2023).

Acknowledgements

We would like to express our gratitude to Miss Siriwan Sriwong, scientist, and Miss Sukanya Maison, animal husbandry technician at the Laboratory Animal Center, Thammasat University, for their excellent assistance in animal care and tissue collection. We also thank Mr. Somkiat Sarachat, an undergraduate medical student at Siam University, for his assistance with behavioral analysis. This study acknowledges the research grant support provided by the Fundamental Fund 2567, Thailand Science Research and Innovation through Siam University, to S.L. (03/2567) and NSTDA, Thailand (P2351510), supported to M.K. and K.N.

Author contributions

S.L. and M.K. conceived the research and designed the experiments. N.R., P.B., K.N., P.W., S.B., N.S., N.C., A.I., and R.S. conducted the investigation and performed data analysis. S.L., K.N., and M.K. provided resources and acquired funding. S.L., A.I., P.W., and M.K. visualized the data and drafted the manuscript. All authors participated in editing the manuscript.

Declarations

Competing interests

The authors declare no competing interests.

Ethics statement

The experimental procedures were approved by the Institutional Animal Care and Use Committee of Thammasat University, Pathum Thani, Thailand (project number 21-2021, renewed in 2024). The study was conducted in compliance with the ARRIVE guidelines (https://arriveguidelines.org).

Additional information

Correspondence and requests for materials should be addressed to M.K.